2019 IEEE 58th Conference on Decision and Control (CDC)
Palais des Congrès et des Expositions Nice Acropolis
Nice, France, December 11-13, 2019

Stability Analysis for a Class of Resource-Aware, Co-Regulated Systems*

Xinkai Zhang and Justin Bradley

***Abstract*— In this paper we develop four methods for proving stability for a subclass of co-regulated systems – finite-state, co-regulated systems with restrictions on possible sampling rates. "Co-regulation" is a control strategy we previously developed wherein cyber and physical effectors are dynamically adjusted in response to holistic system performance. The cyber effector, sampling rate, is adjusted in response to off-nominal conditions in the controlled system, and the physical effector adjusts control outputs corresponding to the current (changing) sampling rate. The resulting computer-control system is a discrete-time-varying system with changing zero-order holds and sampling periods, and unknown delays over discrete intervals. This makes performance guarantees such as stability difficult to obtain.**

We address this difficulty by drawing from specialized results in the control community to develop four methods for proving asymptotic stability of finite-state, co-regulated systems. Each successive method relaxes the assumptions needed to guarantee stability. This lays the groundwork for a more all-encompassing analytical framework for co-regulated systems. We use the results to demonstrate stability for a co-regulated multicopter unmanned aircraft system.

I. Introduction

Cyber-Physical Systems (CPS) host an interacting suite of communication and computational tasks, as well as physical system actuation and sensing. This requires careful allocation of these resources to accomplish mission objectives. For control systems this allocation most often takes the form of fixed-rate controller design with an accompanying fixed-period computational task in a real-time schedule. Part of why this fixed-period control strategy has been so successful is the rich theoretical foundation of both the control [1], [2] and real-time systems (RTS) communities [3], [4] which provide performance guarantees. Other control strategies that carefully allocate resources such as event-triggered control [5], or self-triggered control [6] are still developing a comparable all-encompassing theory. As a result, to provide performance guarantees they tend to rely on less-traditional results from advanced control strategies and then impose limitations on sampling, packet drop rates, delays or other timing characteristics [6]–[8]. Similarly, in the RTS community, alternate scheduling strategies such as rate-adaptive tasks [9], rhythmic tasks [10], or control-driven tasks [11] that attempt to allocate resources on-demand are typically limited to one or a small set of time-varying periodic tasks.

*This work was supported in part by USDA-NIFA 2017-67021-25924 and NSF IIS-1638099

X. Zhang is a graduate student in the Department of Electrical and Computer Engineering, University of Nebraska-Lincoln, USA. xinkai.zhang@huskers.unl.edu

J. Bradley is an Assistant Professor in the Department of Computer Science and Engineering, University of Nebraska-Lincoln, USA. jbradley@cse.unl.edu

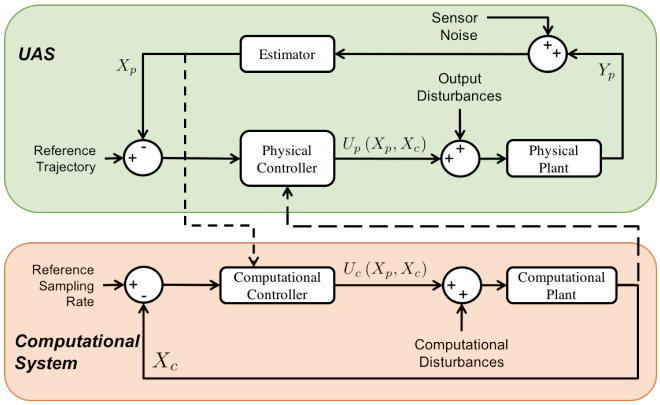

Fig. 1: Co-Regulation Block Diagram

Our approach, co-regulation of cyber and physical effectors, is a method of dynamically adjusting resources and control performance in response to system performance [12], [13], and has been proven effective in simulation [14], and real-system demonstrations [15]. In this strategy, a traditional state-space control model is augmented with a computational model representing sampling rate. Figure 1 shows how this is accomplished in a multicopter Unmanned Aircraft System (UAS) [14]. Output from a cyber model representing sampling rate is fed to the physical controller which adjusts physical system performance accordingly. Simultaneously, output from the physical plant is fed to the cyber controller which adjusts sampling rate in response to physical performance. Discrete-time-varying controllers for both the physical and cyber systems are designed holistically, thereby co-regulating cyber and physical effectors in response to overall system performance. Our work has primarily revolved around cyber-physical vehicles (e.g., multicopters, CubeSats) [14], [15]. Moreover, our strategy has been applied by others in different application domains such as control of grid-tied Active Front End (AFE) power converters [16], loads in active distribution networks [17], and the optimization of plant and controller parameters for an automated electric vehicle [18].

One benefit of our approach is a holistic representation of both the control and real-time computational scheduling systems which lends itself to the goal of an all-encompassing theory providing a resource-aware, co-regulation framework with performance guarantees. However, this is difficult because the computer-controlled system has a dynamically changing sampling rate and thus exhibits discrete-time-varying zero-order holds (ZOH) and sampling periods, as well as delays and holds over potentially unknown discrete intervals. From the perspective of the RTS, the task schedule

978-1-7281-1398-2/19/$31.00 ©2019 IEEE

must dynamically update in response to changing conditions in the physical system while guaranteeing all other deadlines are met. These characteristics don't fit cleanly into an existing modeling paradigm and presents a fundamental challenge in the kind of holistic modeling required by modern computer-controlled systems.

Traditionally, a time-varying sampling period in a computer-controlled system is seen as an aberration resulting from implementation [19], [20], the robustness to which the controller must be examined and designed [21], [22]. Time-varying sampling intervals have been addressed in subclasses of computer-controlled system theory such as network control and hybrid systems [23]. Systems with varying sampling rate can be viewed as time-delay systems [24]–[26], hybrid systems [27], [28], Input/Output interconnections [29], [30], discrete-time systems with time-varying parameters [23]. These results use different analytical frameworks to model and provide results for narrow classes of systems.

Toward the goal of developing an analytical framework providing performance guarantees for co-regulated systems, we develop a series of results for the subclass of finite-state co-regulated systems. Each strategy borrows specialized results from the control systems community, and while increasingly difficult to solve, broadens the scope of the results – laying a foundation for a broader class of co-regulated systems. To solidify the techniques, we apply the proposed strategies to the stability analysis for the co-regulated system we developed for a multicopter Unmanned Aircraft System (UAS) in [14].

The contributions in this paper are:

- development of stability guarantees for the class of finite-state, co-regulated systems, laying a foundation for a broader analytical framework.
- application of these methods to the stability analysis of a co-regulated, multicopter UAS.

With these methods of providing guarantees in place, these contributions will help solidify co-regulation as a viable method to holistically design CPS.

II. Problem Formulation

Co-regulated cyber-physical systems can be represented by an augmented, stacked state-space system as:

$$\begin{aligned} \dot{X}_p &= f_p(t, X_p) + U_p(X_p, X_c) \\ \dot{X}_c &= U_c(X_p, X_c). \end{aligned} \tag{1}$$

where X_p and f_p are the physical system states and dynamics, X_c is the state of the resource, in this case, the control task execution rate (sampling rate) of the system. $U_p(X_p, X_c)$ is the physical control law, and $U_c(X_p, X_c)$ regulates the resource - the sampling rate. Because both are functions of both X_p and X_c, system control performance and sampling rate are directly linked. The co-regulated system is a computer-controlled system, where the sampling rate is dynamically updated, exhibits time-varying zero-order holds (ZOH) and sampling periods, as well as delays and holds over potentially unknown discrete intervals. Throughout this work we will use subscript "p" to indicate the physical system, and subscript "c" to indicate the cyber/computational system.

A. Physical System Model

Our physical model is a quadcopter UAS, whose model is obtained by applying Newton's law or Euler-Lagrange equations [31], [32]. For physical controller design, we linearize the equations about an equilibrium point to obtain a linear state-space model

$$\dot{X}_p = A_p X_p + B_p U_p, \tag{2}$$

where subscript p indicates the model of the physical system. X_p is the state, A_p and B_p are system matrices representing dynamics, and U_p is the control input.

B. Cyber System Model: Sampling Rate

We model the cyber system as a set of task execution rates of mission critical tasks. In a complete co-regulated framework,

$$\dot{X}_c = A_c X_c + B_c U_c$$

would consist of task rates for the complete set of mission critical tasks (e.g., navigation, image processing, communication, control, sensing, planning, etc.) and would be co-regulated alongside, and in response to, system performance. Since the execution rate of tasks other than physical controller will not influence the system stability, in this paper we focus on just the control task sampling rate. We model it as

$$\dot{x}_c = u_c, \tag{3}$$

where x_c is the sampling rate or execution frequency of the computational control task, and u_c acts as a control input to adjust this rate. The sampling rate x_c will increase when the control input u_c is positive, while negative u_c will cause the sampling rate x_c to drop. This single integrator formulation allows control task execution rate to move rapidly in response to the control effort, u_c, similar to how a real-time task schedule might be dynamically manipulated [9], [13].

C. Physical System Control

For digital controller design, we need to discretize the system for a given sampling period. In the most general case, the discrete system matrices may vary due to parameter changes, uncertainty in dynamics, or in our case, a time-varying sampling rate [13]. While we have explored several control strategies for this type of co-regulated system [12]–[14], for a quadcopter Unmanned Aircraft Systems our Gain-Scheduled Discrete Linear Quadratic Regulator (GSDLQR) provides excellent performance [14]. In that strategy, we first define a finite set of fixed sampling rates $f_i (i = 1, 2, 3, \ldots, N)$ as operating points. We assume that f_1 is the lowest sampling rate while f_N is the highest. We then discretize the system at each operating point to obtain corresponding discrete system matrices $\Phi_p[f_i]$ and $\Gamma_p[f_i]$.

Under this approach, all the possible sampling rate values that can be applied for the physical system during runtime are included in a discrete set

$$\Sigma \subseteq \{f_1, f_2, \ldots, f_N\}, \tag{4}$$

where f_1 is given by the minimum rate that can guarantee stable control, and f_N corresponds to the maximum sampling rate corresponding with available slack in the real-time

Rate x_c	Gain $K_p[k]$
$x_c = x_{c,\min}$ Hz	$K_p[k] =$ DLQR @$x_{c,\min}$ Hz
$x_c = 10$ Hz	$K_p[k] =$ DLQR @10 Hz
$x_c = 11$ Hz	$K_p[k] =$ DLQR @11 Hz
⋮	⋮
$x_c = x_{c,\max}$ Hz	$K_p[k] =$ DLQR @$x_{c,\max}$ Hz

TABLE I: GSDLQR at Different Sampling Rates

schedule[1]. The density of the operating points in $[f_1, f_N]$ should be chosen based on modes of the dynamics [1] while ensuring stability. For example, in gain scheduling control, operating points are chosen to be close enough to each other to ensure that the variation of the scheduling variable is "slow" [33]. The theory for choosing "dense enough" operating points is explored in [34]–[36].

Since the sampling rate is dynamically evolving and the discretized physical system model is unique for each sampling rate, the resulting system is a discrete-time-varying system [14]. So the discrete-time system model dynamically changes with the sampling rate applied at each time step. To obtain the system model at each sampling rate, the system is discretized by using a zero order hold (ZOH) approximation, in which the control inputs are held constant between updates. The discrete system at each sampling rate can be obtained by

$$\Phi_p = e^{A_p T_d}, \text{ and } \Gamma_p = \int_0^{T_d} e^{A_p \eta} B_p d\eta. \tag{5}$$

Since we will change the sampling rate dynamically at discrete intervals, the system matrices Φ_p and Γ_p will be recalculated as the sampling rate varies. Thus the system matrices become functions of the time step k. The discrete-time system model is then,

$$X_p[k+1] = \Phi_p[k] X_p[k] + \Gamma_p[k] U_p[k] \tag{6}$$

with control input

$$U_p[k] = -K_p[k] X_p[k]. \tag{7}$$

The design of feedback controllers for a system that can dynamically adjust its own sampling rate is a relatively new area for research [14]. In previous work we employed a discrete-time-varying control strategy by gain scheduling a discrete linear quadratic regulator controller (GSDLQR) at a series of sampling rates [14]. First, we design DLQR controllers for the quadrotor at discrete operating points between the upper and lower bounds, then, we "schedule" the appropriate DLQR gains for the quadrotor corresponding to the commanded sampling rate as in Table I. This paradigm ensures that the DLQR gain used to compute the next control input corresponds with the newly commanded sampling period for the control task.

D. Cyber System Control

For the discrete-time-varying co-regulated system, we have developed a coupled GSDLQR physical system controller, which calculates a gain based on the time-varying sampling rate x_c. A second controller is now needed to calculate the coupled computational control input u_c, which adjusts the sampling rate, in real time, as the dynamics of the system change [14]. In previous work we presented two cyber system control laws [14]. The cyber control law consists of two components. The first component scales the error between the current sampling rate and a desired reference rate. This has the effect of pushing the sampling rate toward the desired reference rate. The second component scales the difference between the current physical state to the reference physical state. This pushes the sampling rate faster to provide better control authority when needed. The computational control law is represented as

$$u_c = G_{cp}\left(X_p - X_{p,ref}\right) - g_c\left(x_c - x_{c,ref}\right).$$

The coupling gain, G_{cp}, is used to increase the sampling rate of the system in response to physical state error. The gain, g_c, drives x_c toward the desired reference sampling rate $x_{c,ref}$. To find cyber gains G_{cp} and g_c, we employ an optimization scheme presented in [14].

The discrete-time cyber control law with respect to time step k is then

$$x_c[k+1] = x_c[k] + \frac{1}{x_c[k]} u_c[k], \tag{8}$$

with control input

$$\begin{aligned} u_c[k] =& G_{cp}\left(X_p[k] - X_{p,ref}[k]\right) \\ & - g_c\left(x_c[k] - x_{c,ref}[k]\right). \end{aligned} \tag{9}$$

However, under this cyber controller the sampling rate could change continuously in the pre-defined interval $f_i \in [f_{\min}, f_{\max}]$, indicating the system will operate under infinitely many possible sampling rates. This leads to difficulty in developing stability guarantees. Here we simplify analysis by changing the structure of our previous cyber controller, and let the sampling rate discretely switch among a finite number of states in the interval. We therefore add a constraint to locate each $x_c[k]$ on the nearest pre-defined operating points:

$$x_c[k] = f_i, \tag{10}$$

where

$$|X_c[k] - f_i| \leq |X_c[k] - f_j| \quad \forall f_i, f_j \in \Sigma. \tag{11}$$

That is, the cyber state (sampling rate), which is decided by the cyber controller, changes discretely in a closed interval with a finite number of different states.

E. Finite-State, Co-regulation Model for Stability Analysis

Combining the physical control model with the cyber control model, a holistic model of finite-state, co-regulated system for stability analysis can be achieved. The system model can be described by

$$X_p[k+1] = A[k] X_p[k] \tag{12}$$

where

$$A[k] = \Phi_p[k] - \Gamma_p[k] K_P[k]. \tag{13}$$

Based on our co-regulation strategies, we first discretize the system at each operating point to obtain $\Phi_p[f_i]$ and $\Gamma_p[f_i]$.

[1]We assume schedule slack is a bounded value that can be obtained before runtime.

We then design a set of controller gains $K_P[f_i]$ which are mapped to a set of fixed sampling rates, where $f_i \in \Sigma$. As a result, $A[k]$ in Equation (13) has a finite number of possible values corresponds to the value of f_i which denotes different operating points. The discrete, closed-loop model in Equation (13) can be represented as

$$\begin{aligned} X_p[k+1] &= A[f_i]X_p[k] \\ A[f_i] &= \Phi_p[f_i] - \Gamma_p[f_i]K_P[f_i] \\ f_i &\in \Sigma. \end{aligned} \tag{14}$$

We define each operating point as an "operating mode" of the co-regulated system. For stability analysis, we treat the finite-state, co-regulated system in Equation (14) as a switched system. A switched system is a dynamical system that consists of a finite number of "subsystems" and a logical rule that orchestrates switching between these subsystems [37]. The physical system at each operating mode can be represented by a subsystem, and the system evolves by switching among different subsystems along a trajectory that is decided by the cyber controller. Therefore, each closed-loop system evolution will be characterized by an infinite product of closed-loop matrices taken from $A[f_i]$, where $f_i \in \Sigma$.

The co-regulated system could be stable or unstable when operating at a single operating mode depending on the system characteristics and the physical controller. For example, in our previous work, a co-regulated system of a small satellite (CubeSat) has unstable operating modes that must be avoided by the co-regulated system [12]. In the case of a co-regulated quadcopter UAS, all the individual operating modes can be exponentially stabilized by a DLQR controller design [14]. However, even when all the subsystems of a switched system are exponentially stable, it is still possible to construct a divergent trajectory from any initial state with a poor switching function [37]. Therefore, the stability of the co-regulated system at each operating mode is not sufficient to assure stability since the system could destabilize under arbitrary operating mode switching.

III. Stability Analysis

In this section, we introduce four different criteria to evaluate the stability for the class of finite-state, co-regulated systems, and provide corresponding proofs.

A. Common Quadratic Lyapunov Functions

This criteria provides a sufficient condition for the stability of finite-state, co-regulated systems based on the existence of Common Quadratic Lyapunov Functions (CQLF).

Theorem 1: The finite-state, co-regulated system (14) is asymptotically stable under arbitrary switching trajectories if all of its operating modes are asymptotically stable and there exists a common positive definite symmetric matrix P for all operating modes that satisfies

$$A^T[f_i]PA[f_i] - P < 0; \quad \forall f_i \in \Sigma. \tag{15}$$

Proof: For the finite-state, co-regulated system (14), we define a candidate Lyapunov function

$$V(X_p[k]) = X_p[k]^T P X_p[k]$$

where $P > 0$. Then

$$\begin{aligned} &V(X_p[k+1]) - V(X_p[k]) \\ &= X_p[k+1]^T P X_p[k+1] - X_p[k]^T P X_p[k] \\ &= X_p[k]^T (A^T[f_i]PA[f_i] - P) X_p[k]. \end{aligned}$$

If the condition in (15) holds, then

$$V(X_p[k+1]) - V(X_p[k]) < 0, \quad \forall f_i \in \Sigma$$

implying the finite-state, co-regulated system is asymptotically stable [37]. ■

The conditions in (15) can be expressed as linear matrix inequalities (LMIs) [38]. The LMI form of (15) is:

$$\begin{bmatrix} A[f_i]^T P A[f_i] - P & 0 \\ 0 & -P \end{bmatrix} > 0, \quad \forall f_i \in \Sigma. \tag{16}$$

The equations in (16) from all operating modes are then combined to form a set of LMIs. If a common solution matrix, P, to the combined LMIs is found, then the condition in Theorem 1 is met and the co-regulated system is stable under arbitrary switching trajectories.

B. Lie Algebraic Approach

Another approach is to provide a Lie algebraic condition for the finite-state, co-regulated system based on the solvability of the Lie algebra generated by the states' matrices. It was shown that if the Lie algebra associated with a family of stable matrices is solvable, then there exists a CQLF [38]. We provide a theorem/proof for application of this concept to a finite-state, co-regulated system.

Theorem 2: The finite-state, co-regulated system (14) is asymptotically stable under arbitrary switching trajectories if all of its operating modes are asymptotically stable and there exists an invertible matrix $T \in \mathbb{C}^{n \times n}$ for all operating modes that satisfies

$$T^{-1}A[f_i]T \text{ is upper triangular}; \quad \forall f_i \in \Sigma. \tag{17}$$

Proof: For the finite-state, co-regulated system (14), we assume (17) is satisfied. Thus there exists an invertible matrix T such that $T^{-1}A[f_i]T$ is upper triangular for $f_i \in \Sigma$. That is, each matrix $A[f_i]$ is similar to an upper triangular matrix under a common similarity transformation T [39]. In matrix terms, the existence of T is equivalent to the argument that the Lie algebra generated by this group of matrices $A[f_i], f_i \in \Sigma$, is solvable [39]. Then, the Lie algebraic solution of the matrices guarantees the existence of a CQLF for the system [38]. Based on Theorem 1, the corresponding finite-state, co-regulated system is asymptotically stable. ■

As an extension to Theorem 1, the Lie algebraic approach provides an alternative way to verify the existence of a CQLF for the finite-state, co-regulated system.

C. Switched Quadratic Lyapunov Functions

This criteria provides a sufficient condition for the stability of finite-state, co-regulated systems based on the existence of Switched Quadratic Lyapunov Functions (SQLF). And similarly, if a SQLF exists for a finite-state, co-regulated system, we can conclude that the system is stable for all switching trajectories.

When compared with the CQLF method, the existence of SQLF is a less conservative condition for stability analysis for switched linear systems [37], [40], [41], and could be used as an alternative way to check the finite-state, co-regulated system stability when the CQLF check fails. Since the structure of the SQLF is more complex, the results proposed in this section can be considered as a tradeoff between highly conservative methods (those using CQLF) and less conservative but numerically hard to check methods [41]. However, the SQLF method provides a stronger stability result in that if a SQLF exists, the switched system is not only asymptotically stable but also exponentially stable [42].

We start with an indicator function

$$\xi(k) = [\xi_1(k), ..., \xi_N(k)]^T \tag{18}$$

where the equation shown below holds

$$\xi_i(k) = \begin{cases} 1, & \text{when system is described by state } A[f_i] \\ 0, & \text{otherwise} \end{cases} \tag{19}$$

$\forall i = 1, ..., N$. Then the finite-state, co-regulated system model denoted by Equation (12) can be represented as:

$$X_p[k+1] = \sum_{i=1}^{N} \xi_i(k) A[f_i] X_p[k] \tag{20}$$

Then we define the switched Lyapunov function as:

$$\begin{aligned} V(X_p[k]) &= X_p[k]^T P\left(\xi(k)\right) X_p[k] \\ &= X_p[k]^T \left(\sum_{i=1}^{N} \xi_i(k) P[f_i] \right) X_p[k] \end{aligned} \tag{21}$$

with $P[f_1], ..., P[f_N]$ symmetric positive-definite matrices. It has been shown that if such a positive definite Lyapunov function exists and

$$\Delta V = V(X_p[k+1]) - V(X_p[k]) < 0 \tag{22}$$

along the solution of Equation (20), then the system is globally asymptotically stable [41].

In the following theorem, we give a necessary and sufficient condition based on LMI for the existence of a Lyapunov function of the form (21) whose difference is negative definite, proving asymptotic stability of the finite-state, co-regulated system. A similar theorem can be found in the switched system research area [41].

Theorem 3: The finite-state, co-regulated system (14) is asymptotically stable under arbitrary switching trajectories if there exists N symmetric matrices $P[f_1], ..., P[f_N]$ satisfying

$$\begin{bmatrix} P[f_i] & A[f_i]^T P[f_j] \\ P[f_j] A[f_i] & P[f_j] \end{bmatrix} > 0, \ \forall f_i, f_j \in \Sigma. \tag{23}$$

Proof: Here we want to prove that if the conditions in (23) are satisfied for all operating modes in a co-regulated system, then there exists a Lyapunov function of the form (21) whose difference is negative definite as (22), thus prove the stability of the co-regulated system.

For the finite-state, co-regulated system (14), we assume (23) is satisfied for all $i = 1, 2, ..., N$ and $j = 1, 2, ..., N$. Now we have a set of N^2 inequalities.

For each i, multiply the $j = 1, 2, ..., N$ inequalities by $\xi_j(k+1)$ and sum, then we can get a result of N inequalities indexed by i:

$$\begin{bmatrix} P[f_1] \sum_{j=1}^{N} \xi_j(k+1) & A[f_1]^T \sum_{j=1}^{N} P[f_j] \xi_j(k+1) \\ A[f_1] \sum_{j=1}^{N} P[f_j] \xi_j(k+1) & \sum_{j=1}^{N} P[f_j] \xi_j(k+1) \end{bmatrix} > 0,$$

$$\begin{bmatrix} P[f_2] \sum_{j=1}^{N} \xi_j(k+1) & A[f_2]^T \sum_{j=1}^{N} P[f_j] \xi_j(k+1) \\ A[f_2] \sum_{j=1}^{N} P[f_j] \xi_j(k+1) & \sum_{j=1}^{N} P[f_j] \xi_j(k+1) \end{bmatrix} > 0,$$

$$\vdots$$

$$\begin{bmatrix} P[f_N] \sum_{j=1}^{N} \xi_j(k+1) & A[f_N]^T \sum_{j=1}^{N} P[f_j] \xi_j(k+1) \\ A[f_N] \sum_{j=1}^{N} P[f_j] \xi_j(k+1) & \sum_{j=1}^{N} P[f_j] \xi_j(k+1) \end{bmatrix} > 0.$$

Then, multiply the resulting $i = 1, 2, ..., N$ inequalities by $\xi_i(k)$ and sum. The result can be denoted as:

$$\begin{bmatrix} \sum_{i=1}^{N} \sum_{j=1}^{N} P[f_i] \xi_j(k+1) \xi_i(k) & \sum_{i=1}^{N} \sum_{j=1}^{N} A[f_i]^T P[f_j] \xi_j(k+1) \xi_i(k) \\ \sum_{i=1}^{N} \sum_{j=1}^{N} A[f_i] P[f_j] \xi_j(k+1) \xi_i(k) & \sum_{i=1}^{N} \sum_{j=1}^{N} P[f_j] \xi_j(k+1) \xi_i(k) \end{bmatrix} > 0.$$

Since $\sum_{i=1}^{N} \xi_i(k) = \sum_{j=1}^{N} \xi_j(k+1) = 1$, we get

$$\begin{bmatrix} \sum_{i=1}^{N} P[f_i] \xi_i(k) & \sum_{i=1}^{N} A[f_i]^T \xi_i(k) \sum_{j=1}^{N} P[f_j] \xi_j(k+1) \\ \sum_{j=1}^{N} P[f_j] \xi_j(k+1) \sum_{i=1}^{N} A[f_i] \xi_i(k) & \sum_{j=1}^{N} P[f_j] \xi_j(k+1) \end{bmatrix} > 0.$$

Based on the definition of the indicator function in (18) (19) (20), we can rewrite the inequality as:

$$\begin{bmatrix} P(\xi(k)) & A^T(\xi(k)) P(\xi(k+1)) \\ P(\xi(k+1)) A(\xi(k)) & P(\xi(k+1)) \end{bmatrix} > 0,$$

which is equivalent by the Schur complement [43] to

$$X_p[k]^T (P(\xi(k)) - A^T(\xi(k)) P(\xi(k+1)) A(\xi(k))) X_p[k] > 0.$$

Then, $\forall X_p[k] \in \mathbb{R}^n$

$$\begin{aligned} \Delta V &= V(X_p[k+1]) - V(X_p[k]) \\ &= -X_p[k]^T (P(\xi(k)) - A^T(\xi(k)) P(\xi(k+1)) A(\xi(k))) X_p[k] < 0. \end{aligned}$$

Thus the co-regulated system is asymptotically stable. ■

We mention that when $P[f_i] = P[f_j]$ for all $f_i, f_j \in \Sigma$, the switched quadratic Lyapunov function becomes the CQLF.

The SQLF method is more flexible in some ways when compared to CQLF method. A SQLF can be used to add restrictions on switching trajectories, such that only stable sequences are allowed. This can be achieved by identifying all possible unstable switching sequences and remove the corresponding unstable state switch from the LMI conditions. As an example, if the switch between f_1 and f_{10} is not stable while all the other switches are stable, a CQLF to verify system stability doesn't exist. However, a SQLF with $i = 1$ and $j = 10$ excluded from Equation (23) can be found and guarantee system stability. This allows us to avoid unstable switches such as those that were found in our co-regulated CubeSat system [12].

D. Minimum Dwelling Time

The CQLF and SQLF methods mentioned above provide sufficient conditions for the stability of finite-state, co-regulated systems under arbitrary switching trajectories. However, while the system may fail to preserve stability under arbitrary switching of the discrete working modes, it may be stable under restricted switching signals. Moreover, based on the cyber controller design, a designer may have prior knowledge about possible switching logic in the co-regulation including restrictions on the switching signals. For example,

there is likely certain bounds on the time intervals between two successive switchings. This could result from the physics of state trajectories that take finite, nonzero time traveling from the initial set to certain guard sets [37]. Such a priori knowledge about the switching signals can allow us to derive stronger stability results for a given finite-state, co-regulated system than in the arbitrary switching case where we use, by necessity, worst case arguments.

The switching trajectories through a set of stable subsystems may cause an unstable result because of the failure to absorb the energy increase caused by switching [44], [45]. By studying the system characteristics when working under different operating modes, we can add constraints to the cyber controller to restrict the switching trajectories to the stability guaranteed switching sequences. The method discussed in this section focuses on the design of time domain restrictions that can be applied to the cyber controller.

Intuitively, in the Minimum Dwell Time (MDT) strategy for finite-state, co-regulated systems, we assume all of the individual operating modes are stable, so that if the system remains in a stable operating mode long enough and switches less frequently one may trade off the energy increase caused by switching and maintain stability [37].

Since for each fixed sampling rate, each discrete-time closed loop system is stable, there exists a Lyapunov function for each system satisfying

$$A^T[f_i]P[f_i]A[f_i] - P[f_i] < 0; \quad \forall f_i \in \Sigma. \tag{24}$$

As an example, assume there are two different operating states of the co-regulated system where the sampling rates are f_1 and f_2, respectively. Define the system when working in the operating mode at a sampling rate f_1 as Σ_1, and similarly define Σ_2 when the sampling rate is f_2. Define two positive definite matrices $P[f_1] > 0$, $P[f_2] > 0$, and assume $P[f_1] > P[f_2]$. We construct a piecewise quadratic Lyapunov function [46] $V(X_p[k])$ as

$$V(X_p[k]) = \begin{cases} X_p[k]^T P[f_1] X_p[k], & \text{when working at } \Sigma_1 \\ X_p[k]^T P[f_2] X_p[k], & \text{when working at } \Sigma_2. \end{cases} \tag{25}$$

Since each mode of the co-regulated system is stable, the Lyapunov function (25) decreases while staying at one operating mode. However, when switching from one operating mode to another, the Lyapunov function might increase [46]. Therefore, to guarantee the overall decrease of the Lyapunov function, the system must remain sufficiently long either with Σ_1 before switching to Σ_2 or with Σ_2 before switching to Σ_1. In this example, since we assume $P[f_1] > P[f_2]$, the Lyapunov function $V(X_p[k])$ decreases when switching from Σ_1 to Σ_2, whereas the Lyapunov function increases when switching from Σ_2 to Σ_1, which can lead to instability.

As illustrated in [46], to guarantee stability, the system should either stay in Σ_2 for at least m sampling intervals before switching or stay in Σ_1 for at least n sampling intervals after switching. In both cases, the decrease in energy along the Lyapunov function during the dwell time in either operating mode is larger than the increase caused by the switch from Σ_2 to Σ_1. Thus, the decrease of the overall piecewise Lyapunov function is ensured resulting in a stable response. We describe this more succinctly in Theorem 4.

Theorem 4: For the finite-state, co-regulated system (14), the switching between any two operating modes, $\forall f_i, f_j \in \Sigma$, is stable if the operating mode at f_i is active for at least n cycles or the operating mode at f_j is active for at least m cycles. The numbers, m and n, are positive integers satisfying

$$(A[f_i]^n)^T P[f_i] A[f_i]^n - P[f_j] < 0 \tag{26}$$

$$(A[f_j]^m)^T P[f_i] A[f_j]^m - P[f_j] < 0, \tag{27}$$

where $P[f_i]$ and $P[f_j]$ are positive definite symmetric matrices satisfying

$$A^T[f_i]P[f_i]A[f_i] - P[f_i] < 0,$$
$$A^T[f_j]P[f_j]A[f_j] - P[f_j] < 0.$$

Here we define the f_i as the lower sampling rate, so $P[f_i] > P[f_j]$.

Proof: We construct a piecewise quadratic Lyapunov function as (25):

$$V(X_p[k]) = \begin{cases} X_p[k]^T P[f_i] X_p[k], & \text{when } f = f_i \\ X_p[k]^T P[f_j] X_p[k], & \text{when } f = f_j. \end{cases} \tag{28}$$

When switching from f_i to f_j,

$$\begin{aligned} \Delta V(X_p[k]) &= V(X_p[k+1]) - V(X_p[k]) \\ &= X_p[k]^T (P[f_i] - P[f_j]) X_p[k]. \end{aligned}$$

Since $P[f_i] > P[f_j]$, $\Delta V(X_p[k]) < 0$, and the system is stable.

When switching from f_j to f_i, we check the value change of the Lyapunov function (25) before and after the switching process. There are two approaches based on the conditions in (26) and (27).

Approach 1: If the system stays in operating mode at f_i for n cycles after switching,

$$\begin{aligned} \Delta V(X_p[k]) &= V(X_p[k+n+1]) - V(X_p[k]) \\ &= X_p[k]^T ((A[f_i]^n)^T P[f_i] A[f_i]^n) X_p[k] - X_p[k]^T P[f_j] X_p[k] \\ &= X_p[k]^T ((A[f_i]^n)^T P[f_i] A[f_i]^n - P[f_j]) X_p[k]. \end{aligned}$$

If the condition in (26) holds, $\Delta V(X_p[k]) < 0$, and the system is stable.

Approach 2: If the system stays in operating mode at f_j for m cycles before switching,

$$\begin{aligned} \Delta V(X_p[k]) &= V(X_p[k+1]) - V(X_p[k-m]) \\ &= X_p[k-m]^T ((A[f_j]^m)^T P[f_i] A[f_j]^m) X_p[k-m] - X_p[k-m]^T P[f_j] X_p[k-m] \\ &= X_p[k-m]^T ((A[f_j]^m)^T P[f_i] A[f_j]^m - P[f_j]) X_p[k-m]. \end{aligned}$$

If the condition in (27) holds, $\Delta V(X_p[k]) < 0$, and the system is stable. ■

The switching trajectory of the sampling rate is decided by the cyber controller (9) of the co-regulated system. Sensible restrictions based on Theorem 4 can be imposed to the scheduling strategy to ensure the stability of each switch. This approach can be applied to the finite-state, co-regulated system by calculating the MDT constraints for each possible switching sequence. For example, suppose that the sampling rates are given as in Equation (4). And $P[f_N]$ is associated with f_N which is the fastest sampling rate. Then the MDT

for all other system sampling rates that can guarantee the stable switching with f_N can be calculated as follows: for all $f_i \in \Sigma$, solve iteratively for each m_i which satisfies

$$(A[f_i]^{m_i})^T P_{f_N} A[f_i]^{m_i} - P_{f_i} < 0. \tag{29}$$

By solving the LMIs, we obtain m_i for each operating mode which can then be included as limitations on the cyber controller or real-time scheduler. The corresponding minimum dwelling times for each possible sampling rate, f_i, are given by ${}^{m_i}/_{f_i}$. Then the stability of the holistic system is guaranteed when switching among sampling rates, f_i.

IV. Discussion

Based on the stability analysis in Section III we present a general discussion about the application of these methods to the stability analysis for finite-state, co-regulated systems.

For finite-state, co-regulated systems with no restrictions on the switching trajectories among operating modes, the existence of CQLF or SQLF can provide a guarantee of system stability for arbitrary switching sequences. The LMI based approach in Theorem 1 and the Lie algebraic approach in Theorem 2 provide two different ways to check the existence of CQLF. The CQLF method has the lowest computational complexity compared with other conditions in this paper, and hence should be tried first. For a co-regulated system with N operating modes, we can check the existence of CQLF by looking for a combined solution from N LMIs or by checking the Lie algebraic solvability of N matrices.

When compared with the CQLF-based method, the SQLF-based method in Theorem 3 is more computationally complex. For a co-regulated system with N operating modes, we need to look for a combined solution from N^2 LMIs to check the existence of SQLF. However, the existence of SQLF is a less conservative condition for finite-state, co-regulated system stability analysis. It could be used as an additional method to check system stability when there does not exist a CQLF for the system. The benefit of these strategies is that the finite-state, co-regulated system can be will be proved to be asymptotically stable under **arbitrary switching trajectories** if any of Theorems 1, 2, or 3 is satisfied.

If the system fails to preserve stability under arbitrary switching, we may still preserve stability under restricted switching sequences. If appropriate timing limitations can be added to the cyber controller, the MDT condtions in Theorem 4 should be followed to find constraints for the cyber controller. In that case the minimum dwelling time for each operating mode under each possible switching sequence can be calculated, and system stability is guaranteed.

A. Stability of Multicopter UAS

We used the stability criteria presented in this paper to verify stability of our co-regulated multicopter UAS [14]. The system state consists of the vehicle's position $\tilde{X}_p = (x, y, z)^T$, orientation in roll ($\phi$), pitch ($\theta$), and yaw ($\psi$) angles, velocity in $\mathbb{R}^3$, and angular rate of change in roll, pitch, and yaw,

$$X_p = \left(x, y, z, \phi, \theta, \psi, \dot{x}, \dot{y}, \dot{z}, \dot{\phi}, \dot{\theta}, \dot{\psi}\right)^T.$$

The input vector, U_p, consists of independent torques in roll (τ_ϕ), pitch (τ_θ), and yaw (τ_ψ), and a net thrust (N)

$$U_p = (\tau_\phi, \tau_\theta, \tau_\psi, N)^T.$$

The physical system model, corresponding to (2), is $\dot{X}_p = \boldsymbol{A}_p X_p + \boldsymbol{B}_p U_p$ where

$$\boldsymbol{A}_p = \begin{bmatrix} & & \mathbf{0}_{6\times6} & & & \mathbb{I}_{6\times6} & & \\ & 0 & g & 0 & \frac{-D_x}{m} & 0 & 0 & \\ \mathbf{0}_{3\times3} & -g & 0 & 0 & 0 & \frac{-D_y}{m} & 0 & \mathbf{0}_{3\times3} \\ & 0 & 0 & 0 & 0 & 0 & \frac{-D_z}{m} & \\ & & \mathbf{0}_{3\times6} & & & \mathbf{0}_{3\times6} & & \end{bmatrix}$$

$$\boldsymbol{B}_p = \begin{bmatrix} & \mathbf{0}_{8\times4} & & \\ 0 & 0 & 0 & 1/m \\ I_{xx}^{-1} & 0 & 0 & 0 \\ 0 & I_{yy}^{-1} & 0 & 0 \\ 0 & 0 & I_{zz}^{-1} & 0 \end{bmatrix}$$

and m and g are the mass of the vehicle and acceleration due to gravity, D_x, D_y, and D_z are the coefficients of drag force acting in each of the coordinate axes, and I_{xx}, I_{yy} and I_{zz} are the inertial moments of the multicopter's body about the pitch, roll and yaw axis respectively. The cyber system model is the same as (3). The GSDLQR controller is designed as shown in Table I and the cyber controller is designed as in (9). We have verified that this co-regulated system satisfies the CQLF and SQLF criteria in Theorems 1, 2, and 3. The satisfaction of either theorem can guarantee the stability of the finite-state, co-regulated system.

V. Conclusion

In this paper, we provide four methods for assessing stability of a subclass of co-regulated systems – finite-state, co-regulated systems. First, a common quadratic Lyapunov function method can be used to check system stability under arbitrary switchings. Second, a condition based on the Lie algebraic solvability of the state matrices group is introduced as an alternative stability criteria. Then, a switched quadratic Lyapunov function criteria is introduced as a less conservative method to evaluate stability while providing its potential value in designing state space restrictions for the cyber controller to guarantee system stability. Finally, a minimum dwelling time method is presented to add time domain restrictions to the cyber controller to achieve stable switching trajectories if the previous tests fail. The two Lyapunov based methods were used to conclude asymptotic stability of the finite-state, co-regulated multicopter UAS system presented in [14].

This work lays the foundation for the penultimate goal of providing a complete analytical framework for co-regulated systems described by Equations (1). Future work will focus on a framework for system stability analysis for the infinite-state, co-regulated systems where the sampling rates are continuously changing. A more complete analytical framework will lead to control synthesis strategies allowing designers to more readily apply co-regulation strategies.

REFERENCES

[1] G. F. Franklin, M. L. Workman, and D. Powell, *Digital Control of Dynamic Systems*. Addison-Wesley Longman Publishing Co., Inc. Boston, MA, USA, 1998.

[2] K. J. Åström and B. Wittenmark, *Computer-controlled systems: theory and design*. Courier Corporation, 2013.

[3] C. M. Krishna and K. G. Shin, *Real-time Systems*. Tata McGraw-Hill Education, 1997.

[4] H. Kopetz, *Real-time systems: design principles for distributed embedded applications*. Springer Science \& Business Media, 2011.

[5] W. Heemels, M. C. F. Donkers, and A. R. Teel, "Periodic event-triggered control for linear systems," *IEEE Transactions on Automatic Control*, vol. 58, no. 4, pp. 847–861, 2013.

[6] W. Heemels, K. H. Johansson, and P. Tabuada, "An introduction to event-triggered and self-triggered control," in *Decision and Control (CDC), 2012 IEEE 51st Annual Conference on*. IEEE, 2012, p. 3270–3285.

[7] K. J. Åström and B. M. Bernhardsson, "Comparison of riemann and lebesgue sampling for first order stochastic systems," in *Decision and Control, 2002, Proceedings of the 41st IEEE Conference on*, vol. 2. IEEE, 2002, p. 2011–2016.

[8] J. P. Hespanha, P. Naghshtabrizi, and Y. Xu, "A survey of recent results in networked control systems," *Proc. of the IEEE*, vol. 95, no. 1, p. 138–162, 2007.

[9] G. C. Buttazzo, E. Bini, and D. Buttle, "Rate-adaptive tasks: Model, analysis, and design issues," in *2014 Design, Automation Test in Europe Conference Exhibition (DATE)*, Mar. 2014, pp. 1–6.

[10] J. Kim, K. Lakshmanan, and R. R. Rajkumar, "Rhythmic tasks: A new task model with continually varying periods for cyber-physical systems," in *Proceedings of the 2012 IEEE/ACM Third International Conference on Cyber-Physical Systems*. IEEE Computer Society, 2012, p. 55–64.

[11] M. Velasco, P. Martí, and E. Bini, "Control-driven tasks: Modeling and analysis," in *2008 Real-Time Systems Symposium*, Nov. 2008, pp. 280–290.

[12] J. M. Bradley and E. M. Atkins, "Coupled cyber-physical system modeling and coregulation of a cubesat," *IEEE Transactions on Robotics*, vol. 31, no. 2, p. 443–456, Apr. 2015.

[13] ——, "Toward continuous state-space regulation of coupled cyber-physical systems," *Proceedings of the IEEE*, vol. 100, no. 1, p. 60–74, Jan. 2012.

[14] X. Zhang, S. Doebbeling, and J. Bradley, "Co-regulation of computational and physical effectors in a quadrotor unmanned aircraft system," in *Proceedings of the 9th ACM/IEEE International Conference on Cyber-Physical Systems*. IEEE Press, 2018, pp. 119–129.

[15] L. Kruse, A. Plowcha, and J. M. Bradley, "Experimental testing and validation of cyber-physical coregulation of a cubesat," in *2018 AIAA SPACE and Astronautics Forum and Exposition*, 2018, p. 5212.

[16] Z. Zhang, Z. Lu, and B. Sun, "Computationally efficient predictive control of grid-tied three-level npc active-front-ends: A cps based solution," in *Chinese Automation Congress (CAC), 2017*. IEEE, 2017, pp. 4622–4627.

[17] Y. Wang, D. Liu, and Q.-S. Li, "A hybrid system based cps model and control of loads in active distribution network," in *Power System Technology (POWERCON), 2016 IEEE International Conference on*. IEEE, 2016, pp. 1–8.

[18] C. Lv, X. Hu, A. Sangiovanni-Vincentelli, C. Marina, Y. Li, and D. Cao, "Driving-style-based co-design optimization of an automated electric vehicle: A cyber-physical system approach," *IEEE Transactions on Industrial Electronics*, 2018.

[19] J. Daafouz and J. Bernussou, "Parameter dependent lyapunov functions for discrete time systems with time varying parametric uncertainties," *Systems & control letters*, vol. 43, no. 5, pp. 355–359, 2001.

[20] B. Anderson and J. B. Moore, "Detectability and stabilizability of time-varying discrete-time linear systems," *SIAM Journal on Control and Optimization*, vol. 19, no. 1, pp. 20–32, 1981.

[21] T. H. Lee, Z.-G. Wu, and J. H. Park, "Synchronization of a complex dynamical network with coupling time-varying delays via sampled-data control," *Applied Mathematics and Computation*, vol. 219, no. 3, pp. 1354–1366, 2012.

[22] N. van de Wouw, P. Naghshtabrizi, M. Cloosterman, and J. P. Hespanha, "Tracking control for sampled-data systems with uncertain time-varying sampling intervals and delays," *International Journal of Robust and Nonlinear Control: IFAC-Affiliated Journal*, vol. 20, no. 4, pp. 387–411, 2010.

[23] L. Hetel, C. Fiter, H. Omran, A. Seuret, E. Fridman, J.-P. Richard, and S. I. Niculescu, "Recent developments on the stability of systems with aperiodic sampling: An overview," *Automatica*, vol. 76, pp. 309–335, 2017.

[24] J. Louisell, "Delay differential systems with time-varying delay: New directions for stability theory," *Kybernetika*, vol. 37, no. 3, pp. 239–251, 2001.

[25] K. Gu, J. Chen, and V. L. Kharitonov, *Stability of time-delay systems*. Springer Science & Business Media, 2003.

[26] C.-Y. Kao and B. Lincoln, "Simple stability criteria for systems with time-varying delays," *Automatica*, vol. 40, no. 8, pp. 1429–1434, 2004.

[27] R. Goebel, R. G. Sanfelice, and A. R. Teel, "Hybrid dynamical systems," *IEEE Control Systems*, vol. 29, no. 2, pp. 28–93, 2009.

[28] ——, *Hybrid Dynamical Systems: modeling, stability, and robustness*. Princeton University Press, 2012.

[29] E. Fridman and U. Shaked, "Input–output approach to stability and l2-gain analysis of systems with time-varying delays," *Systems & Control Letters*, vol. 55, no. 12, pp. 1041–1053, 2006.

[30] C.-Y. Kao and A. Rantzer, "Stability analysis of systems with uncertain time-varying delays," *Automatica*, vol. 43, no. 6, pp. 959–970, 2007.

[31] R. Beard, "Quadrotor dynamics and control rev 0.1," Tech. Rep., 2008. [Online]. Available: http://scholarsarchive.byu.edu/cgi/viewcontent.cgi?article=2324&context=facpub

[32] F. Sabatino, "Quadrotor control: modeling, nonlinearcontrol design, and simulation," 2015.

[33] J. S. Shamma and M. Athans, "Gain scheduling: Potential hazards and possible remedies," *IEEE Control Systems*, vol. 12, no. 3, pp. 101–107, 1992.

[34] W. J. Rugh and J. S. Shamma, "Research on gain scheduling," *Automatica*, vol. 36, no. 10, pp. 1401–1425, 2000.

[35] I. Sardellitti, G. Medrano-Cerda, N. G. Tsagarakis, A. Jafari, and D. G. Caldwell, "A position and stiffness control strategy for variable stiffness actuators," in *Robotics and Automation (ICRA), 2012 IEEE International Conference on*. IEEE, 2012, pp. 2785–2791.

[36] I. Sardellitti, G. A. Medrano-Cerda, N. Tsagarakis, A. Jafari, and D. G. Caldwell, "Gain scheduling control for a class of variable stiffness actuators based on lever mechanisms," *IEEE Transactions on Robotics*, vol. 29, no. 3, pp. 791–798, 2013.

[37] H. Lin and P. J. Antsaklis, "Stability and stabilizability of switched linear systems: a survey of recent results," *IEEE Transactions on Automatic control*, vol. 54, no. 2, pp. 308–322, 2009.

[38] P. Martı, C. Lin, S. A. Brandt, M. Velasco, and J. M. Fuertes, "Draco: Efficient resource management for resource-constrained control tasks," *IEEE Transactions on Computers*, vol. 58, no. 1, pp. 90–105, 2009.

[39] H. Haimovich, J. H. Braslavsky, and F. E. Felicioni, "Feedback stabilization of switching discrete-time systems via lie-algebraic techniques," *IEEE Transactions on Automatic Control*, vol. 56, no. 5, pp. 1129–1135, 2011.

[40] L. Fang, H. Lin, and P. J. Antsaklis, "Stabilization and performance analysis for a class of switched systems," in *Decision and Control, 2004. CDC. 43rd IEEE Conference on*, vol. 3. IEEE, 2004, pp. 3265–3270.

[41] J. Daafouz, P. Riedinger, and C. Iung, "Stability analysis and control synthesis for switched systems: a switched lyapunov function approach," *IEEE transactions on automatic control*, vol. 47, no. 11, pp. 1883–1887, 2002.

[42] A. Kundu and D. Chatterjee, "Stabilizing discrete-time switched linear systems," in *Proceedings of the 17th international conference on Hybrid systems: computation and control*. ACM, 2014, pp. 11–20.

[43] J. Zhang, A. K. Swain, and S. K. Nguang, *Robust Observer-Based Fault Diagnosis for Nonlinear Systems Using MATLAB®*. Springer, 2016.

[44] D. Liberzon and A. S. Morse, "Basic problems in stability and design of switched systems," *IEEE Control systems*, vol. 19, no. 5, pp. 59–70, 1999.

[45] R. A. DeCarlo, M. S. Branicky, S. Pettersson, and B. Lennartson, "Perspectives and results on the stability and stabilizability of hybrid systems," *Proceedings of the IEEE*, vol. 88, no. 7, pp. 1069–1082, 2000.

[46] M. Schinkel and W.-H. Chen, "Control of sampled-data systems with variable sampling rate," *International journal of systems science*, vol. 37, no. 9, pp. 609–618, 2006.